



Pectin/poly(ethylene oxide)/zein/hydroxypropyl methylcellulose acetate succinate-based fibers with nanocellulose for controlled hydroxychloroquine release



Giovana C. Zambuzi ^a, Júlia S. Forster ^a, Davi S.S. Souza ^a, Camilla H.M. Camargos ^{b,c}, Ana C.W. Carvalho ^d, Maíra P. Ferreira ^d, Andreia F. Faria ^e, Camila A. Rezende ^b, Osvaldo de Freitas ^d, Kelly R. Francisco ^{a,f,*}

^a Center for Science and Technologies for Sustainability, Federal University of São Carlos, Sorocaba, SP 18052-780, Brazil

^b Departamento of Physical Chemistry, Institute of Chemistry, Universidade Estadual de Campinas (UNICAMP), Campinas, SP 13083-970, Brazil

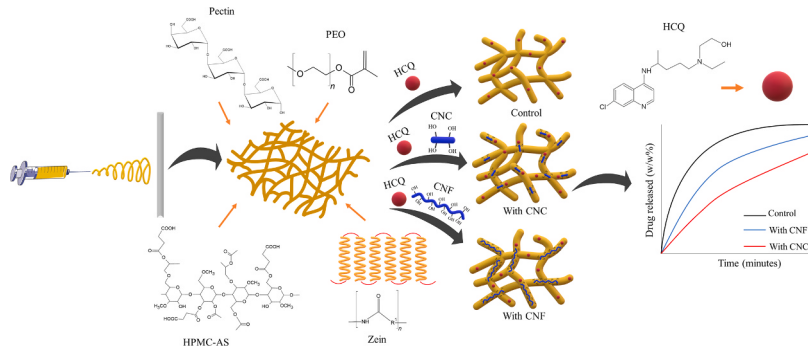
^c School of Fine Arts, Federal University of Minas Gerais (UFMG), Belo Horizonte, MG 31270-901, Brazil

^d Department of Pharmaceutical Sciences, Faculty of Pharmaceutical Sciences of Ribeirão Preto, University of São Paulo, Ribeirão Preto, SP 14040-903, Brazil

^e Engineering School of Sustainable Infrastructure & Environment (ESSIE), Department of Environmental Engineering Sciences, University of Florida, Gainesville, FL, USA

^f Department of Natural Science, Mathematics and Education, Federal University of São Carlos, Araras, SP 13604-900, Brazil

GRAPHICAL ABSTRACT



ARTICLE INFO

Keywords:
Electrospun fibers
Pectin
Zein
Hydroxypropyl methylcellulose acetate succinate
Nanocellulose
Hydroxychloroquine

ABSTRACT

Obtaining new materials for drug delivery through the electrospinning of biopolymers is a strategic approach in the pharmaceutical industry. Incorporating nanoparticles into polymeric matrices influences the morphology of the produced fibers and, consequently, the drug release process. In this study, we produced long cylindrical blended fibers based on pectin, poly(ethylene oxide) (PEO), zein, and hydroxypropyl methylcellulose acetate succinate (HPMCAS) for hydroxychloroquine (HCQ) delivery in the presence of cellulose nanocrystals (CNC) and nanofibrils (CNF). Both CNC and CNF contributed to retaining HCQ in the polymeric matrix for a longer duration, but the CNC-containing fibers had the slowest release rate. The release profiles of HCQ molecules were best fitted using the First Order Model for all types of fibers. The application of the obtained fibers may be of great interest as delivery platforms for HCQ release, particularly in cases such as colon cancer treatment.

* Corresponding author at: Department of Natural Science, Mathematics and Education, Federal University of São Carlos, Araras, SP 13604-900, Brazil.
E-mail address: kfrancisco@ufscar.br (K.R. Francisco).

1. Introduction

Electrospinning is a technique used for preparing fibers with micro- or nanometer diameters by applying a high electrical potential difference between a needle connected to a power supply and a grounded plane electrode [1]. It can be used to fabricate materials for tissue engineering [2–4], catalysis [5], energy storage [6,7], membranes [8,9], and drug release [10,11]. Applications are determined by the fiber characteristics, such as reduced diameter and increased length [12], high surface area [13], chemical composition [14], wettability [15], and mechanical properties [16]. Polymers are widely used to produce electrospun fibers, and employing biopolymers in electrospinning processes is an interesting strategy due to their abundance and relative ease of obtaining biodegradable and biocompatible materials [17], such as zein [18], pectin [19], chitosan [20], and gelatin-based [21] electrospun fibers.

Pectin is a high molecular weight polysaccharide consisting of D-galacturonic acid units abundant in citrus fruit cell walls, where it is the main component [22]. Its versatility allows applications in tissue engineering [23], anticancer treatment [24], food packaging [25], and drug delivery [26], but production of electrified fibers from this biopolymer still faces some challenges [27–29] such as its low jet-forming ability [30]. An alternative to improve this property involves increasing the viscoelasticity of solutions or dispersions by blending pectin chains with other natural or synthetic polymers [30,31].

The addition of poly(ethylene oxide) (PEO), which is a biocompatible and non-toxic polymer with hydrophilic properties [32], improves the electrospinning process. It does so by increasing the viscoelastic properties of the solutions and dispersions, thereby stabilizing the Taylor cone [33–35]. However, fibers produced from pectin and PEO can be solubilized in water, limiting their application in the aqueous phase [31]. In this case, the addition of zein, a hydrophobic polymer, can be used as a complement to produce more water-resistant fibers through the mixture of these polymers [36].

Zein is a protein mainly found in the endosperm of corn grain composed of about 17 amino acids, mostly nonpolar, which contribute to its hydrophobic character [37]. It becomes soluble in alkaline [38] or hydro-alcoholic media, thus allowing the molecule structure to open and form hydrogen bonds, electrostatic and/or van der Waals interactions with the solvent [39]. Zein-based viscoelastic solutions are suitable for electrospinning processes and its fibers can be used for encapsulation [40], food packaging [36,41], and drug delivery [42,43]. Furthermore, obtaining platforms for drug release by blending pectin, PEO, and zein with another polymer that helps pectin in preventing drug crystallization is vital for pharmaceutical applications.

Hydroxypropyl methylcellulose acetate succinate is used mainly in

drug delivery as it inhibits crystallization and improves dispersion stability and solubility of drug molecules [44,45]. In the medicinal area, it has been used to develop nanocontrollers for theophylline release [46] and drug release for colon cancer treatment [47]. Many studies have shown that adding PEO can improve the formation of HPMC or zein polymeric fibers during the electrospinning process [33–35].

Previous studies have shown that pectin in the presence of nanocellulose is a good matrix for delivering hydroxychloroquine (HCQ) molecules from films in a release medium that mimics gastric and colon pH [48]. However, as pectin is highly soluble in aqueous media, the material could not be used for long periods (over 48 h). Zein and hydroxypropyl methylcellulose acetate succinate-based (HPMCAS) electrospun fibers with and without nanofibril cellulose were also investigated as a metronidazole benzoate and metronidazole release platform for periodontal treatment [49]. Results showed that differences in drug and polymeric matrix hydrophilicity can tune the release of the active compound, and nanocelluloses played an important role in the drug release.

Nanocelluloses are versatile bio-based materials that can be extracted through chemical, enzymatic, and mechanical treatments [50]. CNC are usually obtained by acid hydrolysis and are predominantly composed of crystalline domains, resulting in high stiffness [51–53]. Their excellent properties, such as high surface area, reactivity, and self-assembly abilities [54], allow their use in tissue engineering [55, 56], biosensors [57], and drug delivery [58]. CNF are elongated nanostructures composed of both crystalline and amorphous domains commonly obtained by a TEMPO (2,2,6,6-tetramethylpiperidine-1-oxyl radical)-mediated oxidation process followed by mechanical fibrillation [59,60]. Properties such as high surface area, low density, and flexibility [61] enable a wide applicability range, including food packaging [62], coatings [63], electronics [64], and drug delivery [65].

In this scenario, electrospinning blended fibers of pectin, poly(ethylene oxide) (PEO), zein, and HPMCAS that are less soluble than pure pectin in aqueous systems could be more suitable for hydroxychloroquine release due to the arrangement of hydrophilic and hydrophobic polymeric chains. The increment of nanocellulose in the fibers could also modify HCQ release, as observed in a previous work [48].

Hydroxychloroquine (HCQ) is a 4-aminoquinoline, a chloroquine derivative first introduced in the 1950s to treat malaria [66]. Currently, it is also commonly used for treating autoimmune diseases, such as lupus erythematosus [67], rheumatoid arthritis [68], and Sjögren's syndrome [69]. Recent studies have pointed to HCQ as an adjuvant in treating cancer cells, inhibiting cellular autophagy through an increase in lysosomal pH [70]. Other studies have reported on its application in treating lung cancer [71], gastric cancer [72], and colon cancer [73].

In this paper, we aimed to produce cylindrical and defect-free pectin

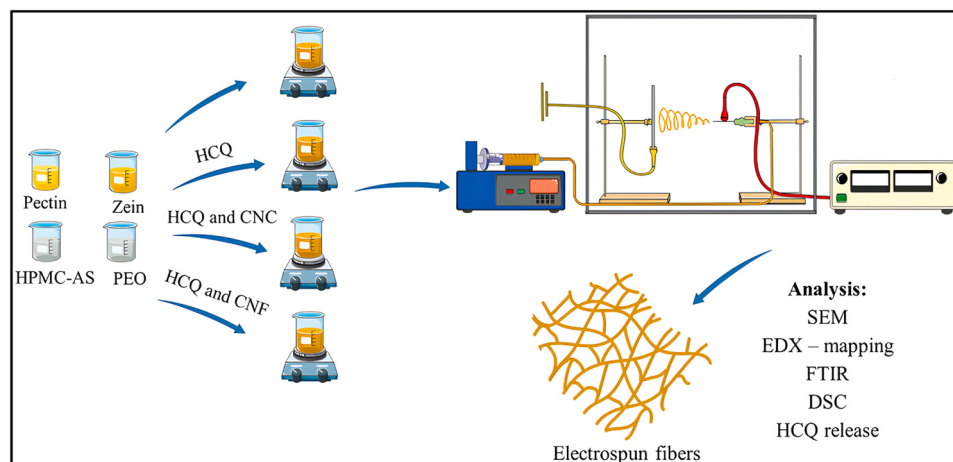


Fig. 1. Schematic illustration of pectin/PEO/zein/HPMC-AS fibers preparation method.

Table 1

Composition (% (w/w)) of pectin/PEO/zein/HPMCAS fibers with and without nanocellulose and HCQ obtained by electrospinning, considering the total amount of components.

Fibers (% (w/w))	HCQ (% (w/w))
5.7 % pectin/22.9 % PEO/28.6 % zein/42.8 % HPMCAS	—
5.5 % pectin/21.8 % PEO/27.3 % zein/41.0 % HPMCAS	4.4 %
5.2 % pectin/20.7 % PEO/25.9 % zein/38.9 % HPMCAS/5.2 % CNC	4.1 %
5.2 % pectin/20.7 % PEO/25.9 % zein/38.9 % HPMCAS/5.2 % CNF	4.1 %

fibers blended with poly(ethylene oxide) (PEO) (used to improve the viscoelasticity of dispersions), zein (added to enhance the fiber water-resistance properties), and hydroxypropyl methylcellulose acetate succinate (HPMCAS) (added to decrease drug crystallization synergistically with pectin) containing hydroxychloroquine (HCQ) by electrospinning. The study examined the impact of adding CNC and CNF on fiber composition and drug release. The fibers were analyzed using FTIR, SEM, and DSC to understand their chemical composition, morphology, and thermal behavior. Drug release in a medium simulating colon pH was studied, and kinetic models of the drug release were developed. The polymer fiber platforms obtained exhibited water resistance and an improved drug delivery profile, with cellulose nanoparticles playing an important role in modulating HCQ release.

2. Experimental section

2.1. Materials

Citrus pectin (Genu® pectin type LM-102 CP Kelco Brazil SA), zein (Sigma® Mv 20 kDa), hydroxypropyl methylcellulose acetate succinate (Ashland® HPMC-AS Mv 100 kDa), and poly(ethylene oxide) (Aldrich® Mv 600 kDa) were used as received. Powder hydroxychloroquine sulfate (HCQ) was purchased from APSEN (Brazil). Nanocelluloses were produced from elephant grass leaves. Cellulose nanocrystals were obtained through conventional acid hydrolysis extraction with sulfuric acid [52, 59], whereas cellulose nanofibrils were obtained by TEMPO-mediated oxidation followed by sonication [52, 59].

2.2. Pectin/PEO/zein/HPMCAS fibers preparation

Solutions of 2 % (w/w) pectin and 8 % (w/w) poly(ethylene oxide) (PEO) were prepared in water. Solutions of 10 % (w/w) zein and 15 % (w/w) hydroxypropyl methylcellulose (HPMCAS) were prepared using a 3:7 (w/w) water/ethanol mixture. All solutions underwent swelling for 24 h, then kept under magnetic stirring at 200 rpm for approximately 10 min for homogenization. The final systems formed by 1 % (w/w) pectin, 4 % (w/w) PEO, 5 % (w/w) zein, 7.5 % (w/w) HPMCAS were mixed for 30 minutes at 200 rpm. For systems containing nanocelluloses, 10 ml of 0.48 % (w/v) CNC or 3 ml of 1.4 % (w/v) CNF were added, resulting in 1 % (w/w) of nanocellulose in the dispersions. After adding 800 mg HCQ to the solutions or dispersions, these were stirred for 30 minutes.

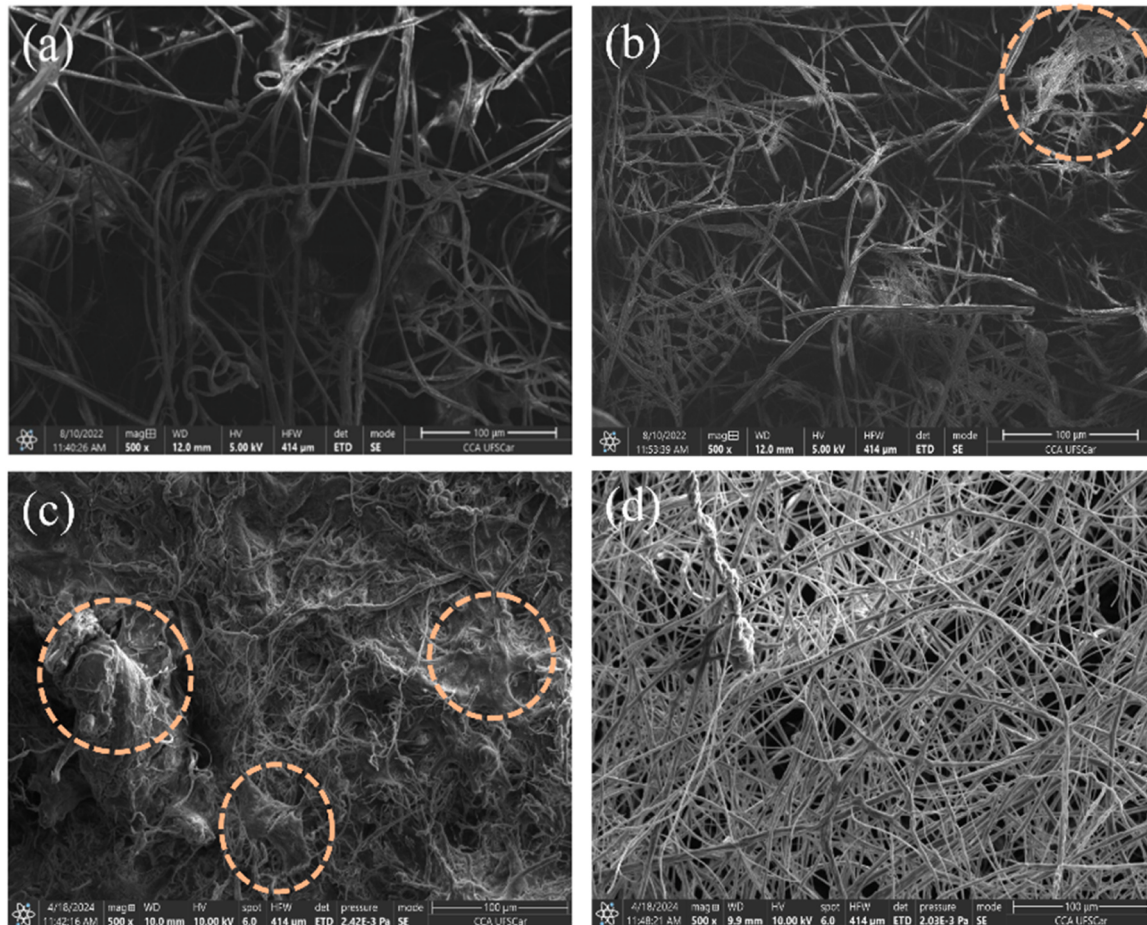


Fig. 2. Micrographs of the electrospun fibers: (a) without HCQ or nanocellulose, (b) with HCQ and without nanocellulose, (c) with HCQ and CNC, (d) with HCQ and CNF. Clusters and agglomerates are indicated by dotted red circles.

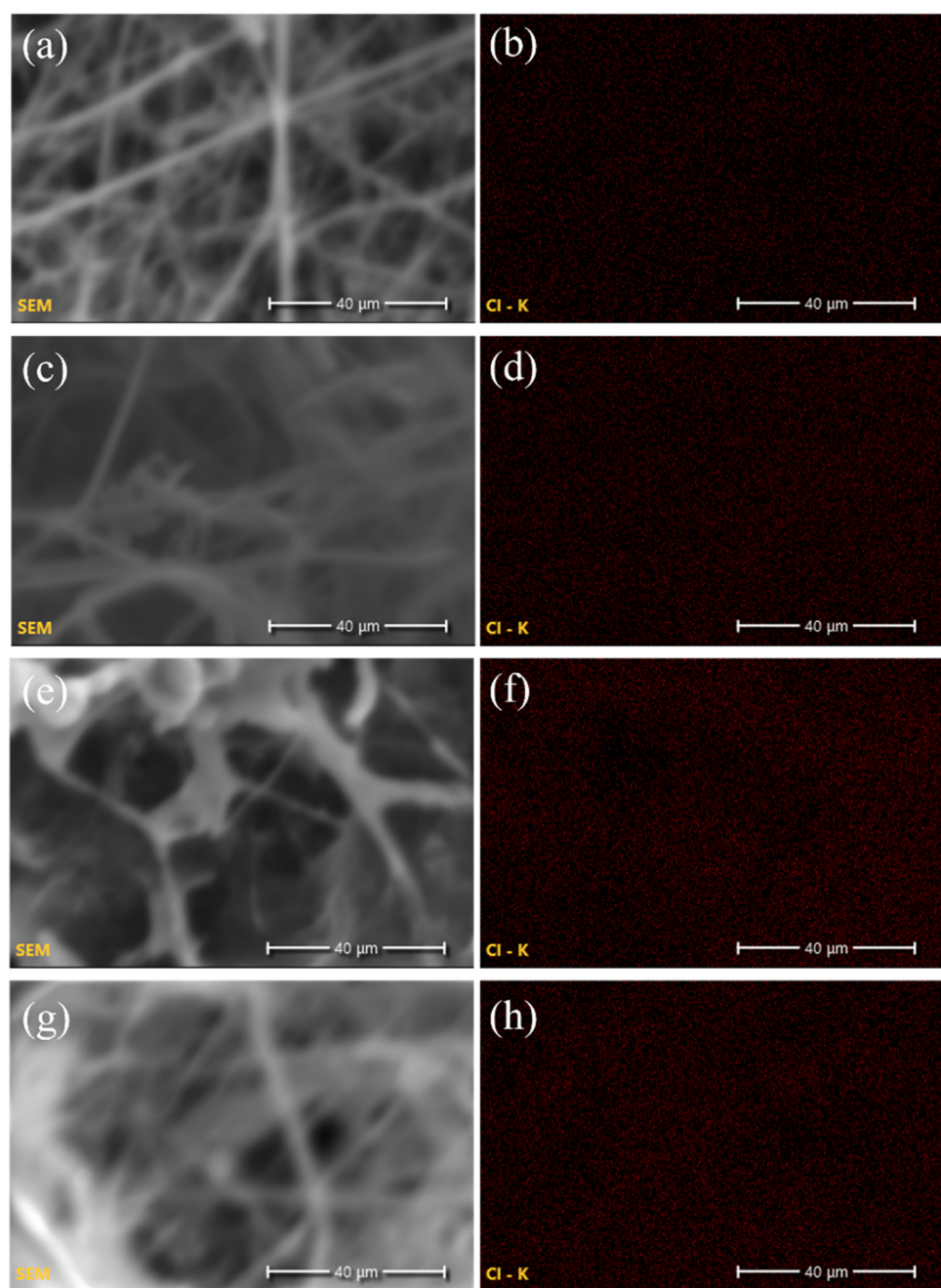


Fig. 3. SEM micrographs and corresponding EDX chlorine mapping of the electrospun fibers: (a and b) without HCQ or nanocellulose, (c and d) with HCQ and without nanocellulose, (e and f) with HCQ and CNC, (g and h) with HCQ and CNF.

Table 2

Element content (in weight %) obtained by EDX-mapping analysis of the electrospun fibers.

Element	Weight %			
	Without HCQ or nanocellulose	With HCQ and without nanocellulose	With HCQ and CNC	With HCQ and CNF
C	60.1	53.3	56.5	59.9
O	37.5	43.5	38.5	36.7
Cl	1.6	2.6	4.5	3.0
Na	0.8	0.7	0.5	0.4

Electrospinning was conducted in a Faraday cage ($1.00 \times 1.00 \times 0.60 \text{ m}^3$) to minimize the influence of external electric fields. Temperature ($25 \pm 2^\circ\text{C}$) and humidity ($55 \pm 1\% \text{ RH}$) were measured using a thermo-hygrometer (MT-242 Minipa). For fiber formation, the solutions were placed in a 60 ml polypropylene syringe (Embramac, Brazil) and pumped under a 4.0 ml/h flow using a syringe pump (Samtronics® 670-39557D/28). A stainless-steel needle of 1.20 mm diameter was used as the upper electrode and connected to the pump by silicone tubes. A 12 kV current was applied using a high voltage source (Spellman CZE1000R), and an aluminum frame ($10 \times 10 \text{ cm}^2$) coated with aluminum foil and positioned at 9 cm from the needle was used as a counter electrode to collect the fibers. The produced fibers were kept in desiccators for at least 48 h before analysis. Fiber solubility was determined by loss of mass due to contact with a buffer solution at pH 6.8, resulting in solubility ranging from 8 to $11 \pm 1.5\% \text{ (w/w)}$ in the first

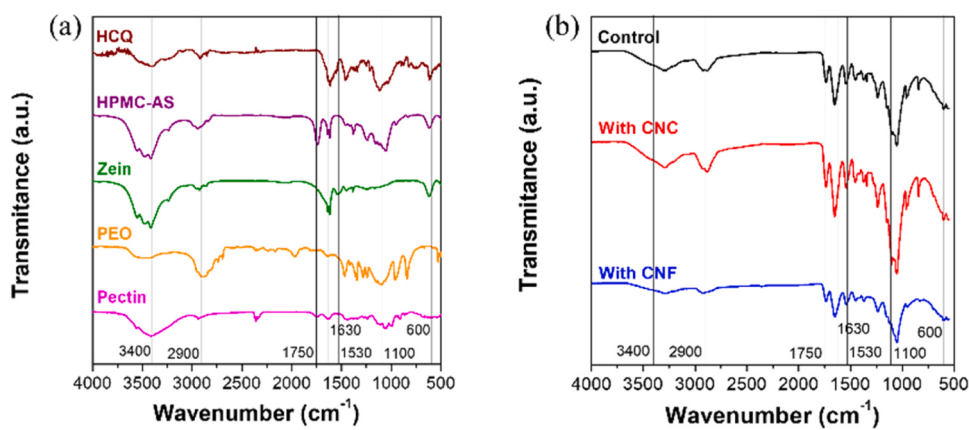


Fig. 4. FTIR spectra of (a) pristine components (HCQ (brown line), HPMC-AS (purple line), zein (olive line), PEO (orange line) and pectin (magenta line)) and (b) the fibers with HCQ (control) (black line) and fibers with HCQ and CNC (red line) or CNF (blue line).

120 minutes and $19\text{--}34 \pm 2\%$ (w/w) after 24 h. The Supplementary Material (Fig. SM1) contains pictures of the electrospinning setup and the produced fibers. The fiber preparation method is illustrated in Fig. 1, and Table 1 presents the final fiber composition.

2.3. Methods

2.3.1. Scanning electron microscopy (SEM)

Fiber images were obtained using a Prisma E (Thermo Scientific®) microscope operating at 15 kV, by secondary electron imaging (SEI) and backscattered electron imaging (BEI). Fibers were deposited in an aluminum sample holder ($1 \times 1 \text{ cm}^2$), fixed with carbon tape and coated with an evaporated palladium-gold alloy using a Bal-Tec MED 020 Sputter. The fiber diameter was determined by measuring 100 random points of two different micrographs (scale bar of $20 \mu\text{m}$) for each sample using the Image J software (imagej.nih.gov).

2.3.2. Fourier transform infrared (FTIR)

FTIR spectra of pectin/zein/HPMCAS/nanocellulose fibers with or without hydroxychloroquine were obtained using a Bruker FT-IR Tensor II spectrometer, operating with KBr insert holder or ATR (attenuated total reflectance) accessory. Spectra were obtained by accumulating 128 scans within the spectral range of $500\text{--}4000 \text{ cm}^{-1}$ with a 4 cm^{-1} resolution.

2.3.3. Differential scanning calorimetry (DSC)

Fiber DSC (approximately 5 mg) hermetically sealed in an aluminum holder were obtained using a PerkinElmer 6000, with temperature ramp starting at -70°C (keeping constant for 10 min), and then heating to 230°C at $10^\circ\text{C min}^{-1}$. Analyses were conducted under a nitrogen atmosphere at a flow rate of 50 ml min^{-1} .

2.3.4. Hydroxychloroquine modified release

Modified HCQ release was conducted using a SOTAX® AT 7 equipment, following the general USP method [74]. Approximately 200 mg of each fiber, corresponding to ca. 8.8 or 8.2 mg of the drug were used for each USP basket apparatus at 37°C and 50 rpm. Phosphate buffer (pH 6.8) was used as a dissolution medium, and 1 ml aliquots of this medium were collected after 15, 30, 45, 60, 120, and 180 min and filtered through a $0.22\text{-}\mu\text{m}$ membrane. HCQ presence was quantified by UV-Vis spectroscopy (Genesys 10 S UV-Vis) at 343 nm and a calibration curve of the same wavelength [75]. Tests were performed in quintuplicate for all fiber samples and under sink conditions.

3. Results and discussion

Morphological analysis of fibers without HCQ or nanocelluloses

(Fig. 2 a) showed a cylindrical shape with smooth surfaces, no beads, and average diameter of $2.09 \pm 0.9 \mu\text{m}$. When hydroxychloroquine is incorporated (Fig. 2 b), but not nanocelluloses, the fibers present a similar morphology with a decreased average diameter of $1.7 \pm 0.5 \mu\text{m}$.

Fibers containing cellulose nanocrystals and HCQ (Fig. 2 c) presented long and rough cylinders with an average diameter of $1.09 \pm 0.5 \mu\text{m}$ and several clusters, which hindered distinguishing separated fibers at certain regions and may stem from the low solvent evaporation during the spinning stage [76]. Fibers containing HCQ and CNF (Fig. 2 d) presented long cylinders and an average diameter of $1.9 \pm 0.7 \mu\text{m}$. Histograms of the fiber diameter are available in the Supplementary Material (Figure SM2).

Chlorine mapping of the fibers (Fig. 3), obtained using SEM coupled with energy-dispersive X-ray spectrometry (SEM EDX-Mapping), showed that this element is distributed throughout the fibers, indicating that HCQ molecules are uniformly dispersed on the polymeric electrospun matrix. SEM EDX-Mapping of other elements present on the fibers can be found on the Supplementary Material (SM3). Table 2 presented the percentage of chlorine and other elements in the fibers, showing that fibers containing HCQ molecules had higher values of the Cl-element, suggesting an effective incorporation of the drug on the fibers.

FTIR spectra of pristine components are shown in Fig. 4 a and they presented the typical bands for the polymers and the drug. Spectra obtained for the HCQ-containing fibers without nanocelluloses (control) and with added CNC and CNF (Fig. 4 b) had similar profiles, showing bands related to HCQ molecules that suggest drug incorporation on the electrospun fibers. The presence of a soft band in the region of $700\text{--}600 \text{ cm}^{-1}$ is attributed to the axial deformation of the drug's C-Cl bond [75]. The band at 3290 cm^{-1} is due to the OH stretching of pectin, PEO, cellulose, and HCQ, and the NH stretching of HCQ and zein [39, 76–78]. This band was shifted to lower wavenumbers (3400 cm^{-1}), suggesting intermolecular interactions among the polymers, nanoparticles, and the drug, mainly due to changes in the hydrogen bond interactions of the produced fibers [37,39]. The band in the 2800 cm^{-1} region is attributed to the C-H stretching of the pectin, PEO, zein, HPMCAS, and HCQ aromatic skeleton [76,79]. The bands at approximately 1740 cm^{-1} are due to carboxyl groups from HPMCAS and pectin. Bands at around 1650 cm^{-1} and at 1544 cm^{-1} are associated with the C=O and COO⁻ stretching of the zein amide I and II groups, respectively [48,79]. These bands were shifted to higher wavenumbers in the fibers compared with zein (bands at 1620 and 1537 cm^{-1} , respectively), which can be explained by the presence of zein in the α -helix structure and an increase of the β -sheets disordered in the fibers [37,79]. The strong band around $1100\text{--}1050 \text{ cm}^{-1}$ is related to the C-O-C stretches of pectin, PEO, and HPMC-AS chains and C-N-C and C-O of HCQ [48,79].

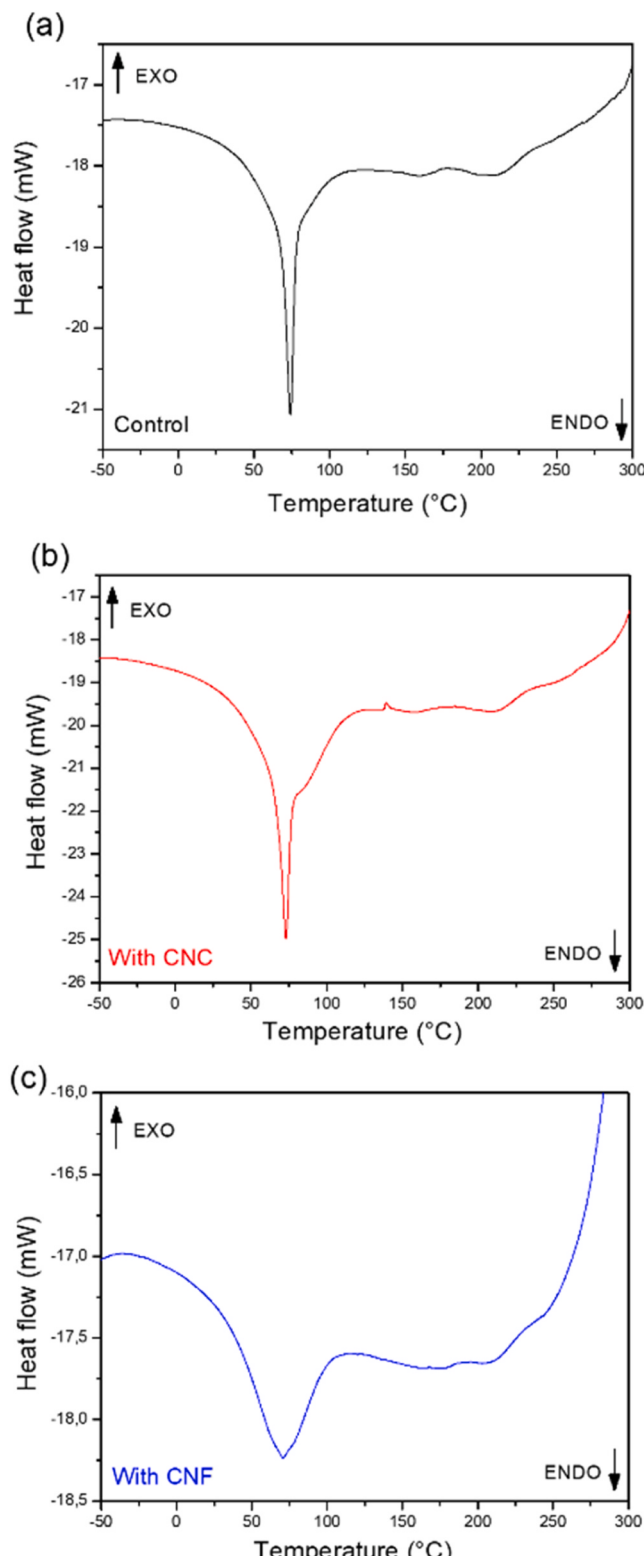


Fig. 5. DSC curves of (a) fibers with HCQ (control), (b) fibers with CNC, and (c) fibers with CNF.

Fig. 5 and Supplementary Material (Fig. SM4) illustrate the DSC thermal analysis of HCQ-loaded fibers and for the pristine components, respectively. DSC curves (**Fig. 3**) were similar for all fibers, showing an endothermic event at around 75 °C related to the evaporation of water molecules unbound in the polymer matrix [80,81]. The two small endothermic shoulders observed at around 150 °C and 210 °C stem from

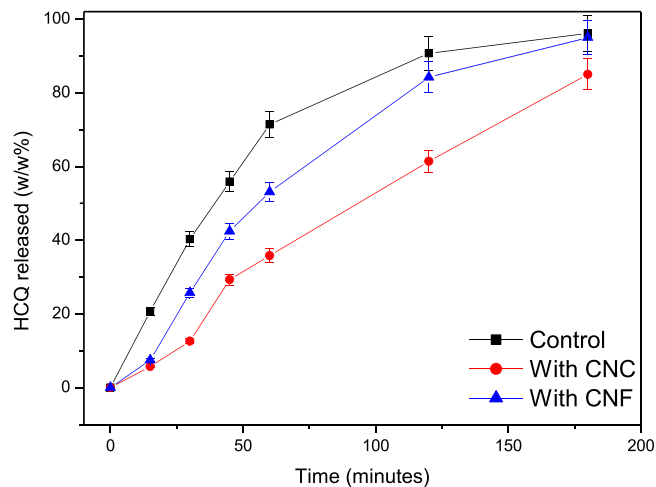


Fig. 6. Release profile of hydroxychloroquine in sodium phosphate buffer (pH 6.8) for pectin/Zein/HPMCAS/HCQ fibers without nanoparticles (control) (black line), with cellulose nanocrystals (red line) and with nanofibrils (blue line).

Table 3

Fitted parameters using First order (using the entire profile) and Korsmeyer-Peppas (using up to 60 % (w/w) release profile) models for HCQ release kinetics.

HCQ release Model	Parameters	Fibers Control	Fibers with CNC	Fibers with CNF
First order	k_1 R^2	0.010 0.993	0.001 0.992	0.002 0.999
Korsmeyer-Peppas	n k_{K-P} R^2	0.481 0.085 0.924	0.880 0.009 0.985	0.688 0.028 0.952

the melting process of HCQ crystals in the fibers, suggesting good interaction with the polymeric matrix given the decreased melting point of the pristine drug observed (reported temperatures of 161 °C and 220 °C, respectively, that can be found in Supplementary Material Fig. SM3) [77,78]. For temperatures above 240 °C, all fibers started to present exothermic events possibly related to molecule degradation.

In comparing the release profiles (**Fig. 6**), we observed that the HCQ-containing fibers without nanoparticles (control) showed a faster release from the beginning, reaching a release of 99 % (w/w) within 180 min which suggests that the formulation came close to the release plateau and thus would be unable to continue releasing the drug for a prolonged period.

Fibers with CNF and CNC showed a slower and similar initial HCQ release in the first 15 min. After 15 min, CNF-containing fibers show a variation of 18.2 % (w/w) in HCQ release between 15 and 30 min, whereas fibers with CNC show a variation of 6.9 % (w/w) and therefore a slower release profile. This difference continues until 120 min. From 120 min to 180 min, drug release from CNF-containing fibers becomes slower with a release variation of 10.8 % (w/w) whereas fibers with CNC show a variation of 23.6 % (w/w). CNF-containing fibers reached a total of 95 % (w/w) HCQ release at 180 min, suggesting that they reached the release plateau. Fibers with CNC, on the other hand, reached a total of 85 % (w/w) HCQ release at 180 min and showed an increasing release profile, indicating that the formulation has the potential to continue drug release after 180 min.

Different parameters can be used to explain the differences in drug release profile. Properties such as porosity, roughness, diameter, and intermolecular interactions between components play a key role in release kinetics. Cellulose nanocrystals have a high surface area that allows to establish strong interactions between the drug and the polymer matrix, providing greater HCQ retention [79]. Similar pattern was

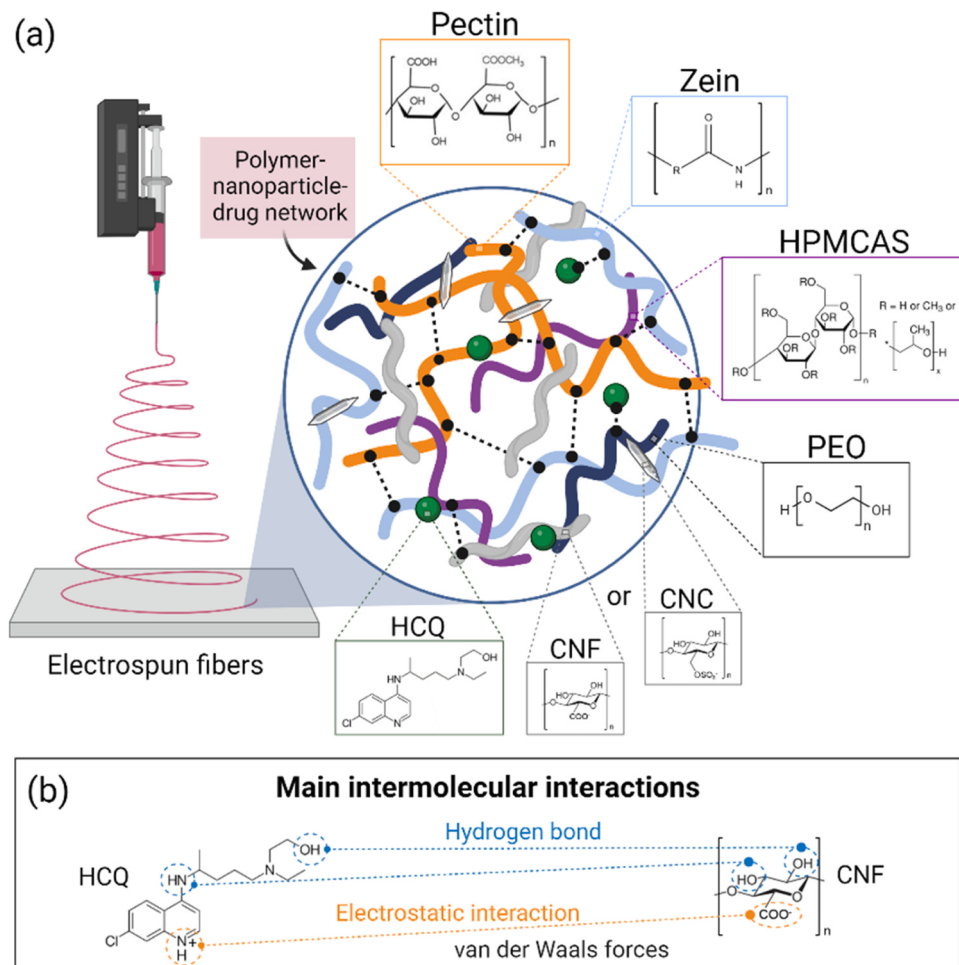


Fig. 7. Schematic representation of (a) the polymeric network within electrospun fibers, illustrating the generic chemical structure of the polymers (pectin, zein, HPMCAS, and PEO), nanoparticles (CNF or CNC), and HCQ. (b) The primary intermolecular interactions in the electrospun fibers, particularly between nanocellulose and HCQ, which may include hydrogen bonds, electrostatic interactions, and van der Waals forces according to the functional groups present in these components.

observed in a previous work which elaborated pectin thin films for modified HCQ release [48]. In comparing the electrospun fibers and pectin films, the former show a slower release rate. At 120 minutes, for example, pectin films at pH 4 released 99 % (w/w) of the drug [48], whereas 65 % (w/w) of HCQ was delivered from pectin/PEO/zein/HPMCAS/CNC fibers. In fact, this new formulation enables a more effective drug delivery as this new platform is less soluble in aqueous medium and has a higher surface area. When aiming for an even slower release mode, pectin/PEO/zein/HPMCAS/nanocellulose fibers are a better option as drug-loading platforms.

The kinetic study of HCQ release from pectin/zein/HPMCAS fibers without and with nanocelluloses used two mathematical models, namely first order (Eq. (1)) and Korsmeyer-Peppas (Eq. (2) [82–84].

$$Q_t = 1 - e^{k_1 t} \quad (1)$$

$$Q_t = k_{K-P} t^n \quad (2)$$

in which Q_t is the fractional drug release at a given time, k_1 and k_{K-P} are the release constants for each release kinetic model, and n is the diffusion exponent. Table 3 shows the values found for these parameters, as well as for the coefficient of determination (R^2).

As can be observed, the model that best fitted the HCQ release process from the fibers in an aqueous medium at pH 6.8 was the First Order model, characterized by the higher R^2 value. This suggests that the release hue does not undergo intumescence, and that drug release occurs by diffusion obeying a proportionality between concentration in the

matrix and in the medium.

Fig. 7 depicts the chemical structure of the components of the electrospun fibers and the potential main molecular interactions between nanocellulose and HCQ within the polymer-nanoparticle-drug network formed through electrospinning. The proposed mechanisms are supported by SEM-EDX chlorine mapping, FTIR data, DSC analysis, and drug release results.

It is expected that pectin, PEO, zein and, HPMC-AS can interact primarily through hydrogen bonds and electrostatic interactions due to the presence of $-OH$, $-COO^-$, and $-NH$ groups in their structures [26,32, 37,44] (Fig. 7(a)). FTIR results for the electrospun fibers exhibited shifts in the bands related to $-OH$, $C=O$, and $-COO^-$ groups, corroborating these intermolecular interactions among the fiber-forming components. Nanocelluloses and HCQ molecules can also interact with each other and with the polymer chains via hydrogen bonds [59,85] (Fig. 7(b)). DSC results indicated that interactions between HCQ molecules became weaker, while EDX chlorine mapping showed that the drug is uniformly distributed on the fibers. Drug release results suggested that HCQ molecules interact more strongly with CNC, leading to slower drug release, compared to CNF. Despite both cellulose nanoparticles having the same backbone chemical structure, CNC are modified with sulfate half-ester groups, while CNF contain carboxylate functional groups [59]. Moreover, the higher specific surface area of CNC compared to CNF, when considering the same amount of nanoparticles added to the systems [59, 63], may explain the enhanced behavior of CNC-containing electrospun fibers. Thus, CNC potentially have more sites to interact with the drug

molecules, explaining the slower drug release in comparison with the drug release profile observed in the other fibers.

4. Conclusion

Our study showed that electrospun pectin/PEO/zein/HPMCAS-based fibers with and without nanocellulose particles for HCQ delivery resulted in long cylindrical microfibers and a few surface defects, using a green solvent to produce the fibers. The drug was uniformly distributed on the fibers and interacted with polymer chains and cellulose nanoparticles mainly via hydrogen bonds and electrostatic interactions. The addition of cellulose nanoparticles (CNC or CNF) can modulate HCQ release profiles, giving an adequate drug release rate. Fibers containing cellulose nanocrystals showed a more efficient release process, ensuring a slower delivery rate, whereas fibers without nanocellulose are recommended for processes requiring a faster drug action. The drug release kinetics for all fibers followed the First Order model. Future research should focus on creating thinner fibers in the nanoscale range, which have larger surface areas, and release the drug over an extended period. To achieve this, changes in the solvent of the electrospun systems, while still using a green solvent, and the development of a polymeric matrix with greater affinity for HCQ molecules should be explored.

CRediT authorship contribution statement

Giovana C. Zambuzi: Writing – original draft, Validation, Methodology, Investigation, Formal analysis, Data curation. **Davi S. S. Souza:** Methodology, Investigation, Formal analysis, Data curation. **Júlia S. Forster:** Methodology, Investigation, Formal analysis, Data curation. **Kelly Francisco:** Writing – original draft, Visualization, Validation, Supervision, Resources, Project administration, Methodology, Investigation, Funding acquisition, Formal analysis, Conceptualization. **Osvaldo de Freitas:** Resources, Funding acquisition, Conceptualization. **Camila A. Rezende:** Writing – original draft, Funding acquisition, Formal analysis. **Ana C. W. Carvalho:** Writing – original draft, Formal analysis. **Camilla H. M. Camargos:** Writing – original draft, Methodology, Investigation, Formal analysis, Data curation. **Andreia F. Faria:** Writing – original draft, Formal analysis. **Maíra P. Ferreira:** Writing – original draft, Formal analysis.

Declaration of Competing Interest

The authors declare no conflict of interest

Data Availability

Data will be made available on request.

Acknowledgements

The authors thank the São Paulo Research Foundation (FAPESP), grants 2017/20006-4 and 2021/12071-6) and the Brazilian Council for Scientific and Technological Development (CNPq, grant 420031/2018-9) for their financial support. Authors G. C. Z and C. H. M. C. hold fellowships from FAPESP (grant 2018/12146-3) and CNPq (grants 140558/2017-9, 151281/2022-0), respectively. We thank Espaço da Escrita - Pró-Reitoria de Pesquisa - UNICAMP for the language services provided

Appendix A. Supporting information

Supplementary data associated with this article can be found in the online version at [doi:10.1016/j.colsurfa.2024.134736](https://doi.org/10.1016/j.colsurfa.2024.134736).

References

- [1] A. Koeiruz, Z.W.V.S. Reddy, Z.K. Nagy, P. Vass, M. Buzgo, S. Ramakrishna, N. Radaci, The history of electrospinning: past, present, and future developments, *Adv. Mater. Technol.* 8 (2023) 2201723, <https://doi.org/10.1002/admt.202201723>.
- [2] S. Nemati, S.J. Kim, Y.M. Shin, H. Shin, Current progress in application of polymeric nanofibers to tissue engineering, *Nano Converg.* 6 (2019), <https://doi.org/10.1186/s40580-019-0209-y>.
- [3] W. Huang, Y. Xiao, X. Shi, Construction of Electrospun Organic/Inorganic Hybrid Nanofibers for Drug Delivery and Tissue Engineering Applications, *Adv. Fiber Mater.* (2019), <https://doi.org/10.1007/s42765-019-00007-w>.
- [4] M. Rahmati, D.K. Mills, A.M. Urbanska, M.R. Saeb, J.R. Venugopal, S. Ramakrishna, M. Mozafari, Electrospinning for tissue engineering applications, *Prog. Mater. Sci.* 117 (2021) 100721, <https://doi.org/10.1002/admt.202201723>.
- [5] S. Li, Z. Cui, D. Li, G. Yue, J. Liu, H. Ding, S. Gao, Y. Zhao, N. Wang, Y. Zhao, Hierarchically structured electrospinning nanofibers for catalysis and energy storage, *Compos. Commun.* 13 (2019), <https://doi.org/10.1016/j.coco.2019.01.008>.
- [6] L. Li, S. Peng, J.K.Y. Lee, D. Ji, M. Srinivasan, S. Ramakrishna, Electrospun hollow nanofibers for advanced secondary batteries, *Nano Energy* 39 (2017) 111–139, <https://doi.org/10.1016/j.nanoen.2017.06.050>.
- [7] Y. Yan, X. Liu, J. Yan, C. Guan, J. Wang, Electrospun nanofibers for new generation flexible energy storage, *Energy Environ. Mater.* 4 (2021) 502–521, <https://doi.org/10.1002/eem.212146>.
- [8] W. Wang, J. Lin, J. Cheng, Z. Cui, J. Si, Q. Wang, X. Peng, L.S. Turng, Dual super-amphiphilic modified cellulose acetate nanofiber membranes with highly efficient oil/water separation and excellent antifouling properties, *J. Hazard. Mater.* 385 (2020) 121582, <https://doi.org/10.1016/j.jhazmat.2019.121582>.
- [9] Y. Yang, P. Peng, Q. Yang, D. Wang, J. Dong, Fabrication of renewable gutta percha/silylated nanofibers membrane for highly effective oil-water emulsions separation, *Appl. Surf. Sci.* 530 (2020) 147163, <https://doi.org/10.1016/j.apsusc.2020.147163>.
- [10] A. Luraghi, F. Peri, L. Moroni, Electrospinning for drug delivery applications: a review, *J. Control. Release* 334 (2021) 463–484, <https://doi.org/10.1016/j.jconrel.2021.03.033>.
- [11] E. Hakkarainen, A. Körkjas, I. Laidmäe, A. Lust, K. Semjonov, K. Kogermann, H. J. Nieminen, A. Salmi, O. Korhonen, E. Haeggström, J. Heinämäki, Comparison of traditional and ultrasound-enhanced electrospinning in fabricating nanofibrous drug delivery systems, *Pharmaceutics* 11 (2019) 495, <https://doi.org/10.3390/pharmaceutics11100495>.
- [12] S. Lei, Z. Quan, H. Zhang, X. Qin, R. Wang, J. Yu, Stable-jet length controlling electrospun fiber radius: Model and experiment, *Polymer* 180 (2019) 121762, <https://doi.org/10.1016/j.polymer.2019.121762>.
- [13] D. Wang, Y. Lian, H. Fu, Q. Zhou, Y. Zheng, H. Zhang, Flexible porous carbon nanofibers derived from cuttlefish ink as self-supporting electrodes for supercapacitors, *J. Power Sources* 599 (2024) 234216, <https://doi.org/10.1016/j.jpowsour.2024.234216>.
- [14] J. Yuan, Q. Chen, C. Fang, S. Zhang, X. Liu, B. Fei, Effect of chemical composition of bamboo fibers on water sorption, *Cellulose* 28 (2021) 7273–7282, <https://doi.org/10.1007/s10570-021-03988-3>.
- [15] C. Lu, J. Wang, X. Lu, T. Zheng, Y. Liu, X. Wang, D. Zhang, D. Seveno, Wettability and interfacial properties of carbon fiber and poly(ether ether ketone) fiber hybrid composite, *ACS Appl. Mater. Interfaces* 11 (2019) 31520–31531, <https://doi.org/10.1021/acsmami.9b00973>.
- [16] A. Anisiei, F. Oancea, L. Marin, Electrospinning of chitosan-based nanofibers: From design to prospective applications, *Rev. Chem. Eng.* 39 (1) (2023), <https://doi.org/10.1515/revec-2021-0003>.
- [17] C.Z. Mosher, P.A.P. Brudnicki, Z. Gong, H.R. Childs, S.W. Lee, R.M. Antrobus, E. C. Fang, T.N. Schiros, H.H. Lu, Green electrospinning for biomaterials and biofabrication, *Biofabrication* 13 (2021) 035049, <https://doi.org/10.1088/1758-5090/ac0964>.
- [18] A. Altan, Ö. Çayır, Encapsulation of carvacrol into ultrafine fibrous zein films via electrospinning for active packaging, *Food Packag. Shelf Life* 26 (2020) 100581, <https://doi.org/10.1016/j.fpsl.2020.100581>.
- [19] S. Chen, S. Cui, H. Zhang, X. Pei, J. Hu, Y.Z. Zhou, Y. Liu, Cross-linked pectin nanofibers with enhanced cell adhesion, *Biomacromolecules* 19 (2) (2018) 490–498, <https://doi.org/10.1021/acs.biomac.7b01605>.
- [20] B.A. Balık, S. Argın, Role of rheology on the formation of Nanofibers from pectin and polyethylene oxide blends, *J. Appl. Polym. Sci.* 137 (2020) 48294, <https://doi.org/10.1002/APP.48294>.
- [21] Y. Wang, Z. Guo, Y. Qian, Z. Zhang, l Lyu, Y. Wang, F. Ye, Study on the electrospinning of gelatin/pullulan composite nanofibers, *Polymers* 11 (2019) 1424, <https://doi.org/10.3390/polym11091424>.
- [22] J.U. Nascimento, G.C. Zambuzi, J.O. Ferreira, J.H. Paula, T.S. Ribeiro, A.L. Souza, C.A. Dreiss, L.L. Silva, K.R. Francisco, A simple process to tune wettability of pectin-modified silanized glass, *Colloids Surf. A: Physicochem. Eng. Asp.* 577 (2019) 67–74, <https://doi.org/10.1016/j.colsurfa.2019.05.056>.
- [23] N.S. Bostancı, S. Büyüksungur, N. Hasircı, A. Tezcaner, Potential of pectin for biomedical applications: a comprehensive review, *J. Biomater. Sci., Polym. Ed.* 33 (14) (2022) 1866–1900, <https://doi.org/10.1080/09205063.2022.2088525>.
- [24] W. Zhang, P. Xu, H. Zhang, Pectin in cancer therapy: a review, *Trends Food Sci. Technol.* 44 (2) (2015) 258–271, <https://doi.org/10.1016/j.tifs.2015.04.001>.
- [25] J. Hung, Z. Hu, L. Hu, G. Li, G. Yao, Y. Hu, Pectin-based active packaging: a critical review on preparation, physical properties and novel application in food

- preservation, *Trends Food Sci. Technol.* 118 (2021) 167–178, <https://doi.org/10.1016/j.tifs.2021.09.026>.
- [26] D.Q. Li, J. Li, H.L. Dong, X. Li, J.Q. Zhang, S. Ramaswamy, F. Xu, Pectin in biomedical and drug delivery applications: a review, *Int. J. Biol. Macromol.* 185 (2021) 49–65, <https://doi.org/10.1016/j.ijbiomac.2021.06.088>.
- [27] S.Z.H. Kiadeh, A. Ghaei, F. Pishbin, J. Nourmohammadi, M. Farokhi, Nanocomposite pectin fibers incorporating folic acid-decorated carbon quantum dots, *Int. J. Biol. Macromol.* 216 (2022) 605–617, <https://doi.org/10.1016/j.ijbiomac.2022.07.031>.
- [28] A. Celebioglu, A.F. Saporito, T. Uyar, Green electrospinning of chitosan/pectin nanofibrous films by the incorporation of cyclodextrin/curcumin inclusion complexes: pH-responsive release and hydrogel features, *ACS Sustain. Chem. Eng.* 10 (14) (2022) 4758–4769, <https://doi.org/10.1021/acssuschemeng.2c00650>.
- [29] C. Xu, J. Ma, W. Wang, Z. Liu, L. Gu, S. Qian, J. Hou, Z. Jiang, Preparation of pectin-based nanofibers encapsulating *Lactobacillus rhamnosus* 1.0320 by electrospinning, *Food Hydrocoll.* 124 (2022) 107216, <https://doi.org/10.1016/j.foodhyd.2021.107216>.
- [30] S. Cui, B. Yao, X. Sun, J. Hu, Y. Zhou, Y. Liu, Reducing the content of carrier polymer in pectin nanofibers by electrospinning at low loading followed with selective washing, *Mater. Sci. Eng. C* 59 (2016) 885–893, <https://doi.org/10.1016/j.msec.2015.10.086>.
- [31] P.L. Rockwell, M.A. Kiechel, J.S. Atchison, L.J. Toth, C.L. Schauer, Various-sourced pectin and polyethylene oxide electrospun fibers, *Carbohydr. Polym.* 107 (2014) 110–118, <https://doi.org/10.1016/j.carbpol.2014.02.026>.
- [32] J.D. Vanza, R.B. Patel, R.R. Dave, M.R. Patel, Polyethylene oxide and its controlled release properties in hydrophilic matrix tablets for oral administration, 1169–1187, *Pharm. Dev. Technol.* 25 (10) (2020) 1169–1187, <https://doi.org/10.1080/10837450.2020.1808015>.
- [33] A. Balogh, B. Farkas, G. Verreck, J. Mensch, E. Borbás, B. Nagy, G. Marosi, Z. K. Nagy, AC and DC electrospinning of hydroxypropylmethylcellulose with polyethylene oxides as secondary polymer for improved drug dissolution, *Int. J. Pharm.* 505 (2016) 159–166, <https://doi.org/10.1016/j.ijpharm.2016.03.024>.
- [34] C. Shi, S. Xi, Y. Han, H. Zhang, J. Liu, Y. Li, Structure, rheology and electrospinning of zein and poly(ethylene oxide) in aqueous ethanol solutions, *Chin. Chem. Lett.* 30 (2019) 305–310, <https://doi.org/10.1016/j.cclet.2018.07.010>.
- [35] A. Akhmetova, G.M. Lanno, K. Kogermann, M. Malmsten, T. Rades, A. Heinz, Highly elastic and water stable zein microfibers as a potential drug delivery system for wound healing, *Pharmaceutics* 12 (2020) 458, <https://doi.org/10.3390/pharmaceutics12050458>.
- [36] B. Niu, L. Zhan, P. Shao, N. Xiang, P. Sun, H. Chen, H. Gao, Electrospinning of zein-ethyl cellulose hybrid nanofibers with improved water resistance for food preservation, *Int. J. Biol. Macromol.* 142 (2020) 592–599, <https://doi.org/10.1016/j.ijbiomac.2019.09.134>.
- [37] E. Corradini, P.S. Curti, A.B. Meniqueti, A.F. Martin, A.F. Rubira, E.C. Muniz, Recent advances in food-packing, pharmaceutical and biomedical applications of zein and zein-based materials, *Int. J. Mol. Sci.* 15 (2014) 22438–22470, <https://doi.org/10.3390/ijms151222438>.
- [38] K. Pan, Q. Zhong, Low energy, organic solvent-free co-assembly of zein and caseinate to prepare stable dispersions, *Food Hydrocoll.* 52 (2016) 600–606, <https://doi.org/10.1016/j.foodhyd.2015.08.014>.
- [39] G.D. Ulrich, A.G. Lemos, A.C. Silva-Alvarez, L.B. Paiva, R.R. Gavioli, L.L. Silva, O. Freitas, K.R. Francisco, Zein/hydroxypropylcellulose biofilms with hydrophilic and hydrophobic montmorillonite clays, *Polym. Compos.* (2023) 1–11, <https://doi.org/10.1002/polb.27266>.
- [40] M.A. Miri, M.B.H. Najafi, J. Movaffagh, B. Ghorani, Encapsulation of ascorbyl palmitate in zein by electrospinning technique, *J. Polym. Environ.* 29 (2021) 1089–1098, <https://doi.org/10.1007/s10924-020-01954-x>.
- [41] W. Jiang, P. Zhao, W. Song, M. Wang, D.G. Yu, Electrospun zein/polyoxyethylene core-sheath ultrathin fibers and their antibacterial food packaging applications, *Biomolecules* 12 (2022) 1110, <https://doi.org/10.3390/biom12081110>.
- [42] C.E. Mariotti, L. Ramos-Rivera, B. Conti, A.R. Boccaccini, Zein-based electrospun fibers containing bioactive glass with antibacterial capabilities, *Macromol. Biosci.* 20 (2020) 2000059, <https://doi.org/10.1002/mabi.202000059>.
- [43] M. Wang, D. Li, J. Li, S. Li, Z. Chen, D.G. Yu, Z. Liu, J.Z. Guo, Electrospun Janus zein-PVP nanofibers provide a two-stage controlled release of poorly water-soluble drugs, *Mater. Des.* 196 (2020) 109075, <https://doi.org/10.1016/j.matdes.2020.109075>.
- [44] Z. Dong, D.S. Choi, Hydroxypropyl Methylcellulose Acetate Succinate: Potential Drug - Excipient Incompatibility, *AAPS PharmSciTech* 9 (3) (2008) 991–997, <https://doi.org/10.1208/s12249-008-9138-5>.
- [45] S.M. Alshahrani, W. Lu, J.B. Park, J.T. Morott, B.B. Alsulays, S. Majumdar, N. Langley, K. Kolter, A. Gryzke, M.A. Repka, Stability-enhanced hot-melt extruded amorphous solid dispersions via combinations of soluplus® and HPMCAS-HF, *AAPS PharmSciTech* 16 (4) (2015) 824–834, <https://doi.org/10.1208/s12249-014-0269-6>.
- [46] M. Liu, Z. Xu, J. Tao, Z. Jia, Y. Wang, Z. Jiang, Nanocontrollers for in vitro drug release based on core-sheath encapsulation of theophylline into hydroxypropyl methylcellulose acetate succinate nanofibers, *J. Vinyl Addit. Technol.* 26 (2020) 566–576, <https://doi.org/10.1002/vnl.21770>.
- [47] H. Li, B. Sanchez-Vazquez, R.P. Trindade, Q. Zou, Y. Mai, L. Dou, L.M. Zhu, G. R. Williams, Electrospun oral formulations for combined photo-chemotherapy of colon cancer, *Colloids Surf. B: Biointerfaces* 183 (2019) 110411, <https://doi.org/10.1016/j.colsurfb.2019.110411>.
- [48] G.C. Zambuzi, C.H.M. Camargos, M.P. Ferreira, C.A. Rezende, O. de Freitas, K. R. Francisco, Modulating the controlled release of hydroxychloroquine mobilized on pectin films through film-forming ph and incorporation of nanocellulose, *Carbohydr. Polym. Technol.* 2 (2021) 100140, <https://doi.org/10.1016/j.carpta.2021.100140>.
- [49] J.O. Ferreira, G.C. Zambuzi, C.H.M. Camargos, A.C.W. Carvalho, M.P. Ferreira, C. A. Rezende, O. Freitas, K.R. Francisco, Zein and hydroxypropyl methylcellulose acetate succinate microfibers combined with metronidazole benzoate and/or metronidazole-incorporated cellulose nanofibrils for potential periodontal treatment, *Int. J. Biol. Macromol.* 261 (2024) 129701, <https://doi.org/10.1016/j.ijbiomac.2024.129701>.
- [50] R. Curvello, V.S. Raghuwanshi, G. Garnier, Engineering nanocellulose hydrogels for biomedical applications, *Adv. Colloid Interface Sci.* 267 (2019) 47–61, <https://doi.org/10.1016/j.cis.2019.03.002>.
- [51] Y.M. Kim, Y.S. Lee, T. Kim, K. Yang, K. Nam, D. Choe, Y.H. Roh, Cationic cellulose nanocrystals complexed with polymeric siRNA for efficient anticancer drug delivery, *Carbohydr. Polym.* 247 (2020) 116684, <https://doi.org/10.1016/j.carbpol.2020.116684>.
- [52] S.A. Nascimento, C.A. Rezende, Combined approaches to obtain cellulose nanocrystals, nanofibrils and fermentable sugars from elephant grass, *Carbohydr. Polym.* 180 (2018) 38–45, <https://doi.org/10.1016/j.carbpol.2017.09.099>.
- [53] V.T. Noronha, C.H.M. Camargos, J.C. Jackson, A.G.S. Filho, A.J. Paula, C. A. Rezende, A.F. Faria, Physical membrane-stress-mediated antimicrobial properties of cellulose nanocrystals, *ACS Sustain. Chem. Eng.* 9 (8) (2021) 3203–3212, <https://doi.org/10.1021/acssuschemeng.0c08317>.
- [54] R. Mu, X. Hong, Y. Ni, Y. Li, J. Pang, Q. Wang, J. Xiao, Y. Zheng, Recent trends and applications of cellulose nanocrystals in food industry, *Trends Food Sci. Technol.* 93 (2019) 136–144, <https://doi.org/10.1016/j.tifs.2019.09.013>.
- [55] S.D. Dutta, J. Hexiu, D.K. Patel, K. Ganguly, K.T. Lim, 3D-printed bioactive and biodegradable hydrogel scaffolds of alginate/gelatin/cellulose nanocrystals for tissue engineering, *Int. J. Biol. Macromol.* 167 (2021) 644–658, <https://doi.org/10.1016/j.ijbiomac.2020.12.011>.
- [56] K. Heise, E. Konturi, Y. Allahverdiyeva, T. Tammelin, M.B. Linder, Nonappa, O. Ikkala, Nanocellulose: recent fundamental advances and emerging biological and biomimicking applications, *Adv. Mater.* 33 (2021) 2004349, <https://doi.org/10.1002/adma.202004349>.
- [57] Z. Ling, F. Xu, J.V. Edwards, N.T. Prevost, S. Nam, B.D. Condon, A.D. French, Nanocellulose as a colorimetric biosensor for effective and facile detection of human neutrophil elastase, *Carbohydr. Polym.* 216 (2019) 360–368, <https://doi.org/10.1016/j.carbpol.2019.04.027>.
- [58] P. Bertsch, L. Schneider, G. Bovone, M.W. Tibbitt, P. Fischer, S. Gstohl, et al., Injectable biocompatible hydrogels from cellulose nanocrystals for locally targeted sustained drug release, *ACS Appl. Mater. Interfaces* 11 (42) (2019) 38578–38585, <https://doi.org/10.1021/acsmami.9b15896>.
- [59] C.H.M. Camargos, C.A. Rezende, Structure-property relationships of cellulose nanocrystals and nanofibrils: implications for the design and performance of nanocomposites and all-nanocellulose systems, *ACS Appl. Nano Mater.* 4 (10) (2021) 10505–10518, <https://doi.org/10.1021/acsnanm.1c02008>.
- [60] T. Saito, S. Kimura, Y. Nishiyama, A. Isogai, Cellulose nanofibers prepared by TEMPO-mediated oxidation of native cellulose, *Biomacromolecules* 8 (8) (2007) 2485–2491, <https://doi.org/10.1021/bm0703970>.
- [61] I. Solala, M.C. Iglesias, M.S. Peresin, On the potential of lignin-containing cellulose nanofibrils (LCNFs): a review on properties and applications, *Cellulose* 27 (2020) 1853–1877, <https://doi.org/10.1007/s10570-019-02899-8>.
- [62] J. Li, F. Zhang, Y. Zhong, Y. Zhao, P. Gao, F. Tian, X. Zhang, R. Zhou, P.J. Cullen, Emerging food packaging applications of cellulose nanocomposites: a review, *Polymers* 14 (2022) 4025, <https://doi.org/10.3390/polym14194025>.
- [63] C.H.M. Camargos, G. Poggi, D. Chelazzi, P. Baglioni, C.A. Rezende, Protective coatings based on cellulose nanofibrils, cellulose nanocrystals, and lignin nanoparticles for the conservation of cellulosic artifacts, *ACS Appl. Nano Mater.* 5 (2022) 13245–13259, <https://doi.org/10.1021/acsnanm.2c02968>.
- [64] S. Nie, N. Hao, K. Zhang, C. Xing, S. Wang, Cellulose nanofibrils-based thermally conductive composites for flexible electronics: a mini review, *Cellulose* 27 (2020) 4173–4187, <https://doi.org/10.1007/s10570-020-03103-y>.
- [65] H. Du, W. Liu, M. Zhang, C. Si, X. Zhang, B. Li, Cellulose nanocrystals and cellulose nanofibrils based hydrogels for biomedical applications, *Carbohydr. Polym.* 209 (2019) 130–144, <https://doi.org/10.1007/s10570-020-03103-y>.
- [66] I. Ben-Zvi, S. Kivity, P. Langevit, Y. Shoenfeld, Hydroxychloroquine: From malaria to autoimmunity, *Clin. Rev. Allergy Immunol.* 42 (2012) 145–153, <https://doi.org/10.1007/s12016-010-8243-x>.
- [67] C. Ponticelli, G. Moroni, Hydroxychloroquine in systemic lupus erythematosus (SLE), *Expert Opin. Drug Saf.* 16 (3) (2017) 411–419, <https://doi.org/10.1080/14704338.2017.1269168>.
- [68] T.S. Sharma, M.C.M. Wasko, X. Tang, D. Vedamurthy, X. Yan, J. Cote, A. Bili, Hydroxychloroquine use is associated with decreased incident cardiovascular events in rheumatoid arthritis patients, *J. Am. Heart Assoc.* 5 (1) (2016) 2016, <https://doi.org/10.1161/JAHA.115.002867>.
- [69] L.J. Dawson, V.L. Caulfield, J.B. Stanbury, A.E. Field, S.E. Christmas, P.M. Smith, Hydroxychloroquine therapy in patients with primary Sjögren's syndrome may improve salivary gland hypofunction by inhibition of glandular cholinesterase, *Rheumatology* 44 (2005) 449–455, <https://doi.org/10.1093/rheumatology/keh506>.
- [70] A. Duffy, J. Le, E. Sausville, A. Emadi, Autophagy modulation: A target for cancer treatment development, *Cancer Chemother. Pharmacol.* 75 (2015) 439–447, <https://doi.org/10.1007/s00280-014-2637-z>.
- [71] Y. Li, F. Cao, M. Li, P. Li, Y. Yu, L. Xiang, T. Xu, J. Lei, Y.Y. Tai, J. Zhu, B. Yang, Y. Jiang, X. Zhang, L. Duo, P. Chen, X. Yu, Hydroxychloroquine induced lung cancer suppression by enhancing chemo-sensitization and promoting the transition

- of M2-TAMs to M1-like macrophages, *J. Exp. Clin. Cancer Res.* 37 (2018) 259, <https://doi.org/10.1186/s13046-018-0938-5>.
- [72] W. Wang, L. Liu, Y. Zhou, Q. Ye, X. Yang, J. Jiang, Z. Ye, F. Gao, X. Tan, G. Zhang, Q. Fang, Z. Xuan, Hydroxychloroquine enhances the antitumor effects of BC001 in gastric cancer, *Int. J. Oncol.* 55 (2) (2019) 405–414, <https://doi.org/10.3892/ijonc.2019.4824>.
- [73] Y. Li, M.H. Cho, S.S. Lee, D.E. Lee, H. Cheong, Y. Choi, Hydroxychloroquine-loaded hollow mesoporous silica nanoparticles for enhanced autophagy inhibition and radiation therapy, *J. Control. Release* 325 (2020) 100–110, <https://doi.org/10.1016/j.jconrel.2020.06.025>.
- [74] United States pharmacopeia 34th ed Rockville (MD): US Pharmacop | Gaba Signaling. (n. d.). Retrieved March 11, 2021, from <https://gabasignaling.com/united-states-pharmacopeia-34th-ed-rockville-md-us-pharmacop/>.
- [75] L.R.M. Ferraz, F.L.A. Santos, P.A. Ferreira, R.T.L. Maia-Junior, T.A. Rosa, S.P. M. Costa, C.M. Melo, L.A. Rolim, P.J. Rolim-Neto, Quality by design in the development and validation of analytical method by ultraviolet-visible spectrophotometry for quantification of hydroxychloroquine sulfate, *Int. J. Pharm. Sci. Res.* 5 (11) (2014) 4666–4676, [https://doi.org/10.13040/IJPSR.0975-8232.5\(11\).4666-76](https://doi.org/10.13040/IJPSR.0975-8232.5(11).4666-76).
- [76] H. Wang, L. Kong, G.R. Ziegler, Fabrication of starch - Nanocellulose composite fibers by electrospinning, *Food Hydrocoll.* 90 (2019) 90–98, <https://doi.org/10.1016/j.foodhyd.2018.11.047>.
- [77] A.N.F. Moraes, L.A.D. Silva, M.A. Oliveira, E.M. Oliveira, T.L. Nascimento, E. M. Lima, I.M.S. Torres, D.G.A. Diniz, Compatibility study of hydroxychloroquine sulfate with pharmaceutical excipients using thermal and nonthermal techniques for the development of hard capsules, *J. Therm. Anal. Calorim.* 140 (2020) 2283–2292, <https://doi.org/10.1007/s10973-019-08953-8>.
- [78] S.M. Hosseini, A. Farmany, M.Y. Alikhani, M. Taheri, S.S. Asi, S. Alamian, M. R. Arabestani, Co-Delivery of Doxycycline and Hydroxychloroquine Using CdTe-Labeled Solid Lipid Nanoparticles for Treatment of Acute and Chronic Brucellosis, *Front. Chem.* 10 (2022) 890252, <https://doi.org/10.3389/fchem.2022.890252>.
- [79] N. Raghav, M.R. Sharma, J.F. Kennedy, Nanocellulose: A mini-review on types and use in drug delivery systems, *Carbohydr. Polym. Technol.* 2 (2021) 100031, <https://doi.org/10.1016/j.carppta.2020.100031>.
- [80] Q. Zhang, Y. Zhao, Y. Zhao, Z. Ding, Z. Fan, H. Zhang, M. Liu, Z. Wang, J. Han, Effect of HPMCAS on recrystallization inhibition of nimodipine solid dispersions prepared by hot-melt extrusion and dissolution enhancement of nimodipine tablets, *Colloids Surf. B: Biointerfaces* 172 (2018) 118–126, <https://doi.org/10.1016/j.colsurfb.2018.08.030>.
- [81] F. Kayaci, T. Uyar, Electrospun zein nanofibers incorporating cyclodextrins, *Carbohydr. Polym.* 90 (2012) 558–568, <https://doi.org/10.1016/j.carbpol.2012.05.078>.
- [82] R.W. Korsmeyer, R. Gurny, E. Doelker, P. Buri, N.A. Peppas, Mechanisms of solute release from porous hydrophilic polymers, *Int. J. Pharm.* 15 (1) (1983) 25–35, [https://doi.org/10.1016/0378-5173\(83\)90064-9](https://doi.org/10.1016/0378-5173(83)90064-9).
- [83] P. Costa, J.M.S. Lobo, Modeling and comparison of dissolution profiles, *Eur. J. Pharm. Sci.* 13 (2001) 123–133, [https://doi.org/10.1016/S0928-0987\(01\)00095-1](https://doi.org/10.1016/S0928-0987(01)00095-1).
- [84] N.A. Peppas, A.R. Khare, Preparation, structure and diffusional behavior of hydrogels in controlled release, *Adv. Drug Deliv. Rev.* 11 (1993) 1–35.
- [85] C.R. Kaiser, K.C. Pais, M.V.N. Souza, J.L. Wardell, S.M.S.V. Wardell, E.R.T. Tiekkink, Assessing the persistence of the N–H/N hydrogen bonding leading to supramolecular chains in molecules related to the anti-malarial drug, chloroquine, *CrystEngComm* 11 (2009) 1133–1140, <https://doi.org/10.1002/10.1039/b823058g>.